COMPARISON OF DUCTILE IRON AND STAINLESS STEEL CASKS AFTER EXTRA-REGULATORY ACCIDENTS*

E.J. Eifert (1), A.S. Heger (1), and P. McConnell (2)

(1) The University of New Mexico, Albuquerque, New Mexico
(2) Sandia National Laboratories, Albuquerque, New Mexico

Summary

This paper presents the results of a series of structural and shielding analyses performed on lead-shielded stainless steel (SS) and ductile iron (DI) casks for transportation and storage of high-level waste (HLW). These analyses were performed to investigate the feasibility of utilizing DI for Type-B transport cask construction by investigating its structural response under severe loading conditions. The analyses have been focused only on rail casks, as it is anticipated that the majority of future HLW inventory will be shipped in that mode. During the structural analyses of the casks, it was found that the lead layer of the lead-shielded stainless steel cask experienced some thinning during the impact. This deformation raised concerns that the cask may fail to meet the shielding requirements as set forth in 10CFR71 (US NRC, 1995). Shielding analyses of the deformed cask are in progress using the analysis code SCALE4.3.

Introduction

Currently the Nuclear Regulatory Commission has only approved SS and ferritic steel as structural materials for containment in Type-B shipping casks. It is generally agreed that SS is a more expensive material with higher manufacturing costs than DI. This economic drawback has motivated this study. At the same time it is known that ferritic materials such as DI have different properties than austenitic stainless steel. Ferritic materials may be subject to brittle fracture, especially at service temperatures near or below the nil-ductility transition temperature when high stresses and/or large pre-service or service-induced flaws are present.

Several analyses of extra-regulatory impacts between two Type-B cylindrical DI and SS casks have been conducted. The simulated drop tests were performed using different combinations and arrangements of casks and consisted of the following four steps:

---

* Sandia is a multiprogram laboratory operated by Sandia Corporation, a Lockheed Martin Company, for the United States Department of Energy under Contract DE-AC04-94 AL85000.

- the target cask lies flat on an unyielding horizontal surface;
- another cask is positioned 9.14 meters above the top surface of the target cask;
- both casks are aligned so that their center lines form a ninety-degree angle when projected onto the horizontal surface; and
- the suspended cask free falls onto the target cask; the target cask remains stationary during free fall.

A sketch of the test set-up is given in Figure 1.

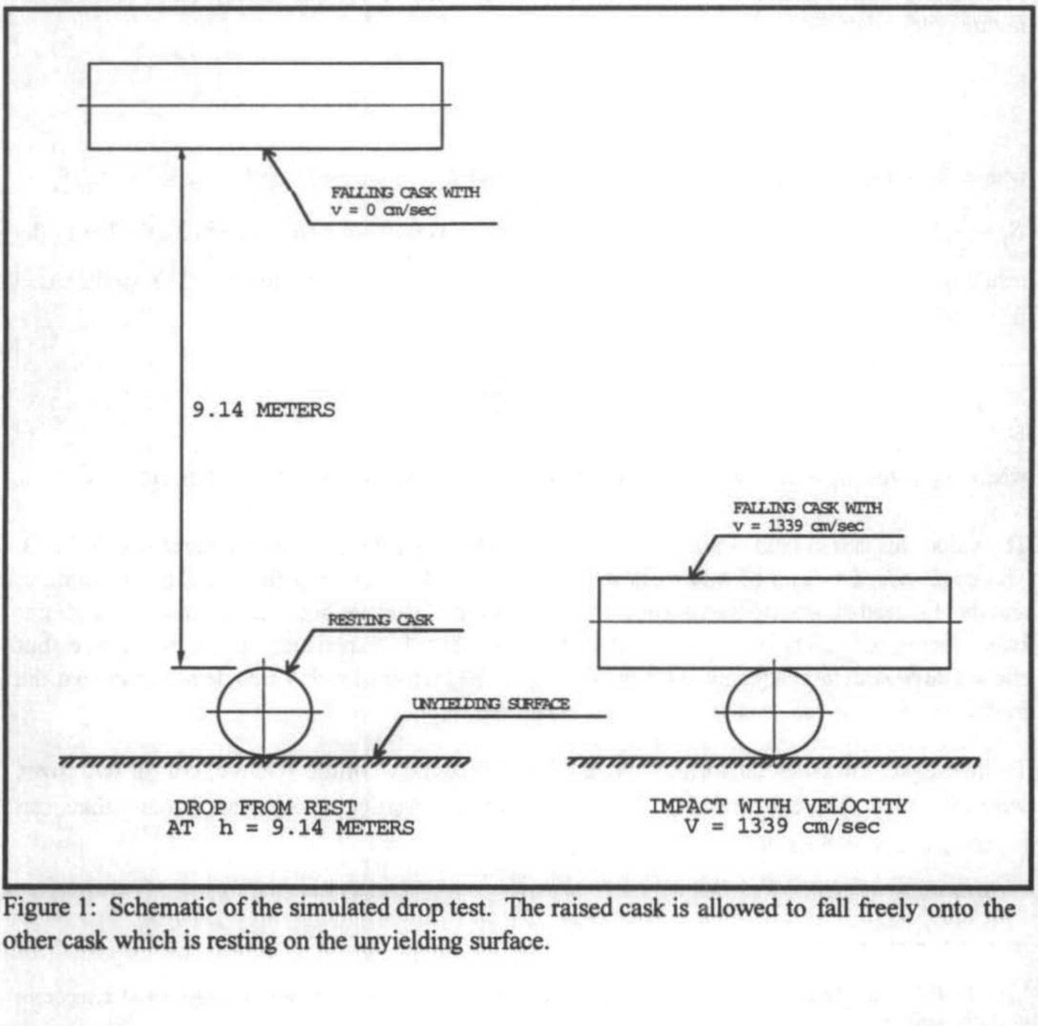

Figure 1: Schematic of the simulated drop test. The raised cask is allowed to fall freely onto the other cask which is resting on the unyielding surface.

Structural Analysis

The investigation into the structural integrity of DI and SS casks under several extra-regulatory conditions have been reported by Burger *et al.* (1995, 1996). A number of additional analyses have been performed to investigate mesh size refinement of the models. A comparison of the data with those reported by Burger *et al.* (1995, 1996) show a slight decrease in the impact duration. There is also an increase in the rebound speeds and final kinetic energies in the drop of the DI onto SS cask and vice versa, while the remainder of the scenarios show a decrease in these values. With two exceptions, the value of permanent plastic deformation increases. The same observation is true for the values of maximum effective plastic strain.

These finite element analysis results, using DYNA-3D (Whirley and Hallquist, 1991), indicate that neither the DI or SS casks experience failure by rupture. Stress- and strain-based factors of safety have been calculated to better compare the obtained results. The plastic stress-based failure criterion is:

$$FS_{\sigma p} = \frac{S_m}{S_a},$$

where S_a is the maximum applied tensile stress, and S_m is defined[1] as the higher of $0.7S_u$ or $S_y + \frac{1}{3}(S_u - S_y)$. The material properties used for the simulations are given in Table 2, and the resulting values for S_m are 362 and 241 MPa for SS and DI, respectively. The strain-based factor of safety is defined as:

$$FS_\varepsilon = \frac{\varepsilon_f}{\varepsilon_a},$$

where ε_a is the maximum true strain in a structure and ε_f is the true strain at failure.

The values for stress- and strain-based factors of safety calculations are summarized in Table 3. The stress-based factors of safety show that neither cask should experience failure by rupture, and that the lead-shielded SS cask has a slight structural advantage over the DI cask. The strain-based factors of safety also show that neither cask should experience failure by rupture, but show a large structural advantage for the DI cask. The factors of safety also demonstrate that the monolithic SS cask has an advantage over the DI cask.

To investigate the potential for the failure of the DI cask by brittle fracture, critical flaw sizes were calculated. The critical flaw size (a_c) for crack propagation, and in turn brittle failure, can be calculated from the following relationship:

---

[1] ASME Boiler and Pressure Vessel Code, Section III, Appendix F for inelastic system analysis and component inelastic analysis

$$a_c = \frac{1}{\pi}\left[\frac{K_{Jc}}{S_a C}\right]^2,$$

where K_{Jc} is fracture toughness, S_a is axial tensile stress, and C is a geometry factor, generally equal to 1.1 to 1.2 (McConnell, 1993). The values for the critical flaw sizes are given in Table 4. The critical flaw sizes calculated for the DI casks are well above those detectable by current inspection techniques.

In one analysis, the lead layer experienced a reduction in thickness of up to 0.56 cm as a result of the impact. This observation has led to a series of shielding analyses to investigate if the Pb-shielded SS cask meets the shielding requirements set forth by 10CFR71 following this extra-regulatory impact.

Shielding Analysis

Section 71.47 of 10CFR71 prescribes that the radiation level does not exceed 2 mSv per hour at any point on the external surface of a package or 0.1 mSv per hour at a point one meter from its external surface. The observed reduction in the thickness of the lead shield of the SS cask during the extra-regulatory drop test could be significant enough to exceed these limits. Therefore, the shielding code SCALE4.3 will be used to investigate the effect of this deformation. SCALE is the Standardized Computer Analyses for Licensing Evaluation and consists of a number of different modules that perform criticality and shielding analysis (ORNL, 95). The code was designed to provide standardized sequences where the user has few analysis options in addition to the geometry model and materials. The SAS4 module, a Monte Carlo cask shielding analysis module using an automated biasing procedure, is being used to perform the shielding analysis (Tang, 1995).

The results from Tang and Hoffman (1988) were used to benchmark the SAS4 module of the SCALE code. They present the results of neutron and gamma dose rates in the axial and radial directions for both a depleted uranium and cast-iron cask. In addition, plans are to calculate the dose rates from the casks used in the structural analysis prior to deformation. These results will be compared to those of Bucholz (1983), who determined the cask dimensions required for a number of cask designs based on shielding, criticality, decay-heat removal, and weight restrictions. Next, the deformed mesh of the lead-shielded SS cask will be modeled to determine the increase in neutron and gamma ray doses. The dose rates, both at the surface of the deformed area and one meter from it, will be calculated and compared to the allowable dose rates.

Conclusions

In all the cases considered in this work, plastic deformation after the impact was observed due to the impact, but was not large enough to cause failure by rupture. The data show better structural performance of monolithic DI casks over sandwich SS/Pb casks with respect to the strain-based factors of safety, while the stress-based factors of safety are comparable for both casks, the slight edge goes to the SS/Pb cask. For the other simulations the monolithic SS cask demonstrates an advantage over the DI cask. Shielding analyses of the SS/Pb cask after impact could point to yet another advantage of the DI cask due to lead thinning in the SS/Pb cask during the impact.

Based on these observations, DI can meet the stringent requirements set forth for materials used in the construction of transport casks. The most obvious benefit of qualifying DI for use in transport casks results in reduction of the use of expensive containment material such as stainless steel. The ability to partially or completely eliminate such material may lead to substantial economic gains through lower material and fabrication costs.

References

Bucholz, J. Scoping Design Analysis for Optimizing Shipping Casks Containing 1, 2, 3, 5, 7 or 10-Year Old PWR Spent Fuel. Oak Ridge National Laboratory, ORNL/CSD/TM-149, TTC-0316 (January 1983)

Burger, C.S. *et al*. Comparison of the Structural Integrity of Ductile Iron and Stainless Steel Casks for Transport Radioactive Material. *International Journal of Radioactive Materials Transport* 7:4 257-263 (1996)

Burger, C.S. *et al*. Comparison of Structural Integrity of Ductile Cast Iron and Lead-Shielded Stainless Steel Casks for Transportation and Storage of Spent Fuel. *PATRAM '95, Packaging and Transportation of Radioactive Materials* (December 1995)

McConnell, P. *et al*. An Evaluation of the Use of Depleted Uranium As a Structural Component for Transport Casks. *Nuclear Technology*, **104**, pp. 171-181 (November 1993)

SCALE: A Modular Code System for Performing Standardized Computer Analyses of Licensing Evaluation. NUREG/CR-0200 (ORNL/NUREG/CSD-2) U.S. Nuclear Regulatory Commission (1995)

Tang, J.S., and T.J. Hoffman. Monte Carlo Shielding Analyses Using an Automated Biasing Procedure. *Nuclear Science and Engineering*: **99**, pp. 329-342 (1988)

Tang, J.S. SAS4: A Monte Carlo Cask Shielding Analysis Module Using an Automated Biasing Procedure. Oak Ridge National Laboratory, ORNL/NUREG/CSD-2/V2/R5 (September 1995)

U.S. Nuclear Regulatory Commission, Regulatory Guide 7.6 "Design Criteria for the Structural Analysis of Shipping Cask Containment Vessels, Rev. 1," (March 1978)

U.S. Nuclear Regulatory Commission, United States Code of Federal Regulations, Title 10, Part 71. Packaging and Transportation of Radioactive Material. (January 1, 1995)

Whirley, R.G. and J.O. Hallquist. DYNA3D: A Nonlinear, Explicit, Three-Dimensional Finite Element Code for Solid and Structural Mechanics - User Manual. University of California, Lawrence Livermore National Laboratory, UCRL-MA-107254 (1991)

Table 1: Summary of simulated drop-test data

Models	DI onto SS	SS onto DI	DI onto SS/Pb (tied interface)	SS/Pb onto DI (tied interface)	DI onto SS/Pb (sliding interface)	SS/Pb onto DI (sliding interface)
Impact duration (s)	0.020	0.016	0.070	0.060	0.085	0.075
Rebound speed (m/s)	3.0	3.9	4.2	4.3	2.2	2.5
Permanent plastic deformation (cm)	2.24 (DI)	2.72 (DI)	0.02 (DI)	0.03 (DI)	0.01 (DI)	0.01 (DI)
	5.23 (SS)	5.72 (SS)	24.5 (SS/Pb)	24.3 (SS/Pb)	52.3 (SS/Pb)	48.0 (SS/Pb)
Maximum effective plastic strain (%)	6.59 (DI)	7.03 (DI)	0.24 (DI)	0.22 (DI)	0.01 (DI)	0.01 (DI)
	11.8 (SS)	11.3 (SS)	13.7 (SS)	10.9 (SS)	11.9 (SS)	11.8 (SS)
	-	-	59.4 (Pb)	59.0 (Pb)	0.05 (Pb)	0.20 (Pb)
Maximum K.E. (kJ)	1245	1258	1245	1190	1245	1190
Final K.E. (kJ)	63	113	122	124	36	38

Table 2: Material properties for DI, SS, and Pb

Material	DI	SS	Pb
Young's Modulus E (10^3MPa)	172	193	0.19
Poisson's Ratio ν	0.27	0.27	0.42
Yield Strength S_y (MPa)	207	207	30
Ultimate Strength S_u (MPa)	310	517	-
Tangent Modulus[2] E_T (10^2MPa)	7.10	15.3	0.165
Total Elongation (%)	12	40	-
Density ρ (g/cm^3)	7.2	8.02	11.3
Fracture Toughness, K_{Jc} ($\mathrm{MPa}\cdot\sqrt{\mathrm{m}}$) @-29°C	73.8	-	-

[2] The tangent modulus is the slope of the inelastic part of a uniaxial stress vs. strain curve (Whirley, 1991, page 73).

Table 3: Factors of safety during simulated impact

	FS_{σ_p} for ASME Design Stress Intensity		FS_{ε} for True Strain Failure Criterion	
	DI	SS	DI	SS
DI onto SS	0.91	1.21	1.82	3.40
SS onto DI	0.90	1.23	1.71	3.53
DI onto SS/Pb (merged)	1.15	1.16	50.0	2.92
SS/Pb onto DI (merged)	1.15	1.24	54.6	3.67
DI onto SS/Pb (sliding)	1.16	1.21	1200.0	3.36
SS/Pb onto DI (sliding)	1.16	1.21	1200.0	3.39

Table 4: Minimum critical flaws of the DI casks calculated from the finite element results

Casks	DI-SS	SS-DI	DI-SS/Pb (nodes merged)	SS/Pb-DI (nodes merged)	DI-SS/Pb (sliding interfaces)	SS/Pb-DI (sliding interfaces)
Critical flaw (cm)	2.06	2.01	3.28	3.28	3.34	3.34
Applied Stress (MPa)	263.6	267.3	209.1	208.9	207.1	207.1

SESSION 5.4

Safety Culture
Public Perception